Available online at www.sciencedirect.com
ScienceDirect
Spectrochimica Acta Part A 69 (2008) 56–61
SPECTROCHIMICA ACTA PART A
www.elsevier.com/locate/saa

Synthesis, spectral characterization and eukaryotic DNA degradation of thiosemicarbazones and their platinum(IV) complexes

G.A. Al-Hazmi [a], N.M. El-Metwally [b], O.A. El-Gammal [b], A.A. El-Asmy [b,*]

[a] *Chemistry Department, Faculty of Science, Taiz University, Taiz, Yemen*
[b] *Chemistry Department, Faculty of Science, Mansoura University, Mansoura, Egypt*

Received 20 December 2006; received in revised form 22 February 2007; accepted 9 March 2007

Abstract

The condensation products of acetophenone (or its derivatives), salicylaldehyde and *o*-hydroxy-*p*-methoxybenzophenone with thiosemicarbazide and ethyl- or phenyl-thiosemicarbazide are the investigated thiosemicarbazones. Their reactions with H_2PtCl_6 produced Pt(IV) complexes characterized by elemental, thermal, mass, IR and electronic spectral studies. The coordination modes were found mononegative bidentate in the acetophenone derivatives and binegative tridentate in the salicylaldehyde derivatives. The complexes were analyzed thermogravimetrically and found highly stable. Some ligands and their complexes were screened against *Sarcina* sp. and *E. coli* using the cup-diffusion technique. [Pt(*o*HAT)(OH)Cl] shows higher activity against *E. coli* than the other compounds. The degradation power of the tested compounds on the calf thymus DNA supports their selectivity against bacteria and not against the human or related eukaryotic organisms.

Keywords: Pt(IV) complexes; Mass spectra; Thermal analysis; Biological activity

1. Introduction

An interesting point for investigating thiosemicarbazones and their complexes is the antimicrobial activity; the reported work shows a high dependence on their substituents [1–4]. Several of thiosemicarbazones have been used for metal ion determination. The previous studies focused on their structural elucidation [5–9]. Recently, thiosemicarbazones were reported involving their complexes with different metal ions [10–14].

In this work, substituted thiosemicarbazones (Scheme 1) and their Pt(IV) complexes were prepared, characterized and screened for their biological activity.

2. Experimental

Reagent grade (BDH) materials and solvents were purified according to the reported methods [15]. Platinum metal purchased from Merck was used in the preparation of H_2PtCl_6. All other chemicals were used without further purification.

2.1. Preparation of the ligands

The investigated ligands were prepared as previously reported [13]. The synthesis of *o*-hydroxyacetophenone thiosemicarbazone (H_2*o*HAT) was explained in detail as an example. 1:1 molar amounts of *o*-hydroxyacetophenone (20 mL, 0.1 mol) and ethanolic solution (30 mL) of thiosemicarbazide (9.1 g, 0.1 mol) were heated for 2 h under reflux on a water bath. Drops of glacial acetic acid were added at the onset of the reflux. The precipitate thus formed was removed by filtration, recrystallized from absolute ethanol and dried. The purity was checked by TLC. The yield of the prepared ligands was found in the range 65–80%. Identification of the ligands was confirmed by IR spectra, ^{1}H NMR and mass spectra.

2.2. Preparation of Pt(IV) complexes

The complexes were prepared by heating 0.01 mol from each ligand and [H_2PtCl_6] in 50 mL aqueous ethanol (v/v) solution with the addition of 0.5 g of sodium acetate to raise the medium pH. The reaction mixture was heated under reflux for 4 h. The precipitate thus formed was filtered off, washed several times with ethanol and diethylether then dried. As an example, the preparation of [Pt(AET)Cl_3][$PtCl_4$] is described in detail. To

* Corresponding author. Tel.: +20 101645966.
E-mail address: aelasmy@yahoo.com (A.A. El-Asmy).

1386-1425/$ – see front matter © 2007 Elsevier B.V. All rights reserved.
doi:10.1016/j.saa.2007.03.010

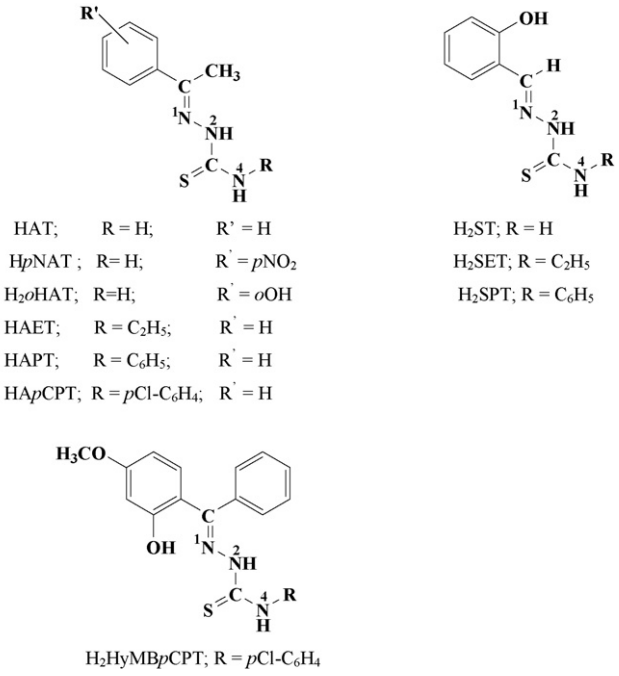

Scheme 1. Structure of thiosemicarbazones.

50 mL reaction flask, add 0.22 g (1 mmol) of 1-acetophenone-4-ethylthiosemicarbazone dissolved in 20 mL ethanol and 0.4 g (1 mmol) of H_2PtCl_6, dissolved in 20 mL distilled H_2O. 0.5 g of sodium acetate is added to the reaction and heated under reflux on a water bath for 2 h. The precipitate thus formed is removed by filtration, washed with distilled water and ethanol then dried in an oven at 90 °C.

2.3. Physical measurements

The infrared spectra were recorded as KBr discs on a Mattson 5000 FTIR Spectrophotometer. The ^{1}H NMR spectra in d_6-DMSO were recorded on a Varian Gemini Spectrometer (200 MHz) at Cairo University. The UV/vis spectra were recorded on UV_2 Unicam UV/vis Spectrophotometer using 1 cm path length quartz cuvette with a stopper. Thermogravimetric curves (TGA and DrTG, 20–1000 °C) were recorded on a Shimadzu thermogravimetric analyzer, TGA-50. The nitrogen flow and heating rate were 20 mL/min and 10 °C/min, respectively, using α-Al_2O_3 as reference. The pH-metric titrations were performed using a Metrohm E536 potentiograph equipped with a 665 DOSIMAT (Metrohm, Herisau, Switzerland). The combined glass electrode was standardized using buffer solutions produced by Fisher's, NJ, USA. Carbon and hydrogen content for the investigated complexes was determined at the Microanalytical Unit, Cairo University, Egypt. Pt(IV) and Cl contents were determined by the well-known methods [16].

2.4. Antimicrobial activity

The ligands and complexes were screened against *Sarcina* sp. as Gram-positive and *E. coli* as Gram-negative bacteria using the cup-diffusion technique [17]. A 0.2 mL of each (10 μg/mL) was placed in the specified cup made in the nutrient agar medium on which a culture of the tested bacteria has been spread to produce uniform growth. After 24 h incubation at 37 °C, the diameter of inhibition zone was measured as mm.

2.5. Genotoxicity

A solution of 2 mg of calf thymus DNA was dissolved in 1 mL of sterile distilled water. Stock concentrations of the investigated ligands and their complexes were prepared by dissolving 2 mg/mL DMSO. An equal volume of each compound and DNA were mixed thoroughly and kept at room temperature for 2–3 h. The effect of the chemicals on the DNA was analyzed by agarose gel electrophoresis. A 2 μL of loading dye was added to 15 μL of the DNA mixture before being loaded into the well of an agarose gel. The loaded mixtures were fractionated by electrophoresis, visualized by UV and photographed.

3. Results and discussion

The reaction between HAT, HAET, HAPT, HA*p*CPT, H_2*o*HATS, H*p*NATS, H_2ST, H_2SET, H_2SPT or H_2HyMB*p*CPT (Scheme 1) and H_2PtCl_6 yields complexes that have different formulae, are stable in air, insoluble in water and common

Table 1
Physical properties, elemental analysis and formula weights of the complexes

Complex/formula	Formula weight		Color	Yield (%)	mp (°C)	Found (Calcd.) (%)		
	Found[a]	Calcd.				C	H	Pt
$[Pt(AT)_2(H_2O)_2]Cl_2$, $C_{18}H_{24}PtN_6O_2S_2Cl_2$	688	689.0	Brown	83		32.0 (31.4)	3.4 (3.5)	28.7 (28.4)
$[Pt(AET)Cl_3][PtCl_4]$, $C_{11}H_{14}Pt_2N_3SCl_5$	–	789.6	Brown	80	>300	17.1 (16.7)	1.9 (1.8)	49.4 (49.5)
$[Pt(APT)(H_2O)(C_2H_5OH)Cl_2]Cl$, $C_{17}H_{22}PtN_3O_2SCl_3$	–	634.3	Brown	78	>300	33.0 (32.2)	3.8 (3.5)	30.1 (30.8)
$[Pt(ApClPT)Cl_3]H_2O$, $C_{16}H_{19}PtN_3O_3SCl_3$	–	599.8	Brown	81	>300	32.6 (32.0)	3.8 (3.2)	32.9 (32.6)
$[Pt(pNAT)Cl_3(H_2O)]$, $C_9H_{11}N_4O_3SPtCl_3$	554	556.6	Yellowish brown	77	>300	19.3 (19.4)	1.8 (2.0)	35.5 (35.1)
$[Pt(oHAT)(OH)Cl]$, $C_9H_{10}N_3O_2SPtCl$	451	452.8	Brown	60	>300	24.2 (23.9)	2.0 (2.2)	43.5 (43.1)
$[Pt(ST)(OH)Cl]0.5H_2O$, $C_8H_9PtN_3O_{2.5}SCl$	450	450.2	Brown	71	>300	20.1 (21.3)	1.9 (2.0)	43.2 (43.4)
$[Pt(H_2SET)Cl_3]Cl{\cdot}3H_2O$, $C_{10}H_{18}PtN_3O_4SCl_4$	623	623.7	Brown	86	>300	18.9 (19.3)	2.0 (2.9)	31.2 (31.3)
$[Pt(SPT)(C_2H_5OH)Cl_2]$, $C_{16}H_{19}PtN_3O_2SCl_2$	577	577.8	Brown	81	>300	33.2 (33.3)	3.1 (2.3)	33.7 (33.8)
$[Pt(HyMBPT)Cl_2]$, $C_{21}H_{17}PtN_3O_2SCl_2$	640	641.7	Brown	75	>300	39.5 (39.3)	2.7 (2.6)	30.6 (30.5)

[a] Values obtained from mass spectra.

organic solvents, but are completely soluble in DMF and DMSO. Their elemental analyses are presented in Table 1.

3.1. IR spectral studies

The important IR bands of the ligands and their complexes are summarized in Table 2. The data reveal the formation of two types of chelates. The ligands in the first type behave as mononegative bidentate and coordinate through the azomethine (C=N) and thiol (C–S) groups; $[Pt(AT)_2(H_2O)_2]Cl_2$, $[Pt(AET)Cl_3][PtCl_4]$, $[Pt(APT)(H_2O)(C_2H_5OH)Cl_2]Cl$, $[Pt(pNAT)Cl_3(H_2O)]$ and $[Pt(ApCPT)Cl_3]H_2O$ are the complexes of this type. The bonding sites are assigned based on the disappearance of $\nu(N^2H)$, the appearance of a new band due to $\nu(C{=}N)^*$ at the same position for the $\nu(C{=}N)_{thio}$, the shift of $\nu(C{=}N)$ to lower frequency [18] by 9–54 cm^{-1} (coordination of the azomethine nitrogen is also consistent with the presence of a new band at 402–462 cm^{-1}, assignable to ν(M–N) [19] vibration) and finally the thioamide band (IV) is absent with the appearance of new bands at 606–656 and 346–370 cm^{-1} due to ν(C–S) [20] and ν(M–S) vibrations, respectively. The reduction of thioamide band (III) observed at 970 cm^{-1} is possible if the coordination occurs both through N and S atoms. The bands observed at 485 and 506 cm^{-1} in the spectra of $[Pt(AT)_2(H_2O)_2]Cl_2$, $[Pt(pNAT)Cl_3(H_2O)]$ and $[Pt(APT)(H_2O)(C_2H_5OH)Cl_2]Cl$ are assigned to ν(M–O) of the coordinated water or the ethanol OH. The band observed at 260–330 cm^{-1} in the chloro complexes is due to ν(M–Cl) [21]. Furthermore, the signal observed at 12.07 ppm (s, 1H) in the ^1H NMR spectrum of $[Pt(APT)(H_2O)(C_2H_5OH)Cl_2]Cl$ may be due to the ethanol OH proton where the broad signal at 4.849 ppm (br) is due to the coordinated water molecule.

The second mode of chelation was found through C=N, C–S and deprotonated phenolic OH in which the ligand acts as binegative tridentate. This behavior is found in the complexes $[Pt(ST)(OH)Cl]0.5H_2O$, $[Pt(SPT)(C_2H_5OH)Cl_2]$, $[Pt(oHAT)(OH)Cl]$ and $[Pt(HyMBPT)Cl_2]$. Elucidation of this mode is proposed by: (i) the disappearance of $\nu(N^2H)$; (ii) the shift of $\nu(C{=}N)$ bands by 9–83 cm^{-1} to lower frequency; (iii) the phenolic oxygen of these ligands, after deprotonation, occupies the third coordination site by the disappearance of ν(OH) band; (iv) the band at 485–505 cm^{-1} in the spectra of the complexes is assignable to ν(Pt–O); (v) the disappearance of $\nu(C{=}S)$ at 778–835 cm^{-1} in the complex spectra with the appearance of new bands at 606–638, 345–370 and 405–453 cm^{-1} due to ν(C–S), ν(Pt–S) and ν(Pt–N), gave an evidence for S, N and O donors. In the spectrum of $[Pt(ST)(OH)Cl]0.5H_2O$, the doublet strong bands at 3451 and 3422 may be due to the ν(OH) vibrations of the two OH; the second is due to the ν(OH) that exists in the ligand. Strong evidence for the presence of OH in $[Pt(ST)(OH)Cl]0.5H_2O$ comes from its ^1H NMR spectrum which shows a signal at 11.18 ppm (s, 1H).

3.2. UV and visible spectra

The solution and solid state spectra are more or less the same indicating that the solvent has little effect on the

Table 2
Assignments of the characteristic IR spectral bands of the ligands and their complexes (cm^{-1})

Compound	$\nu(NH_2)$	ν(OH)	$\nu(N^4H)$	$\nu(N^2H)$	$\nu(C{=}N)$	$\nu(C{=}S)$	ν(C–S)	δOH	ν(Pt–O)	ν(Pt–N)	ν(Pt–S)
$[Pt(AT)_2(H_2O)_2]Cl_2$	3415 (3409)	3441	–	–	1611	–	606	1330	485	402	–
	3368 (3367)	(–)		(3223)	(1628)	(790)	(–)	(–)	(–)	(–)	
$[Pt(AET)Cl_3][PtCl_4]$	–	–	3320	–	1630 (1630)	–	624	–	513	462	370
			(3330)	(3223)	1586 (–)	(788)	(–)		(–)	(–)	(–)
$[Pt(APT)(H_2O)(C_2H_5OH)Cl_2]Cl$	–	–	3322	–	1595	–	610	–	–	405	352
			(3299)	(3250)	(1605)	(794)	(–)			(–)	(–)
$[Pt(ApClPT)(H_2O)Cl_3]$	–	3387	3290	–	1616	–	656	1390	506	446	–
		(–)	(3292)	(3242)	(1635)	(797)	(–)	(–)	(–)	(–)	
$[Pt(ST)(OH)Cl]0.5H_2O$	3209	3451	–	–	1622	–	618	1327 (1366)	486	–	352
	(3371, 3317)	(3442)	(3166)	(3140)	(1611)	(788)	(–)		(–)		(–)
$[Pt(H_2SET)Cl_3]Cl{\cdot}3H_2O$	–	3420	3365	3199	1598	780	–	–	506	446	346
		(3418)	(3282)	(3192)	(1607)	(791)	(–)		(–)	(–)	(–)
$[Pt(SPT)(C_2H_5OH)Cl_2]$	–	–	3363	–	1597	–	638	1373 (1389)	492	412	–
		(3381)	(3352)	(3146)	(1621)	(835)	(–)		(–)	(–)	
$[Pt(HyMBPT)Cl_2]$	–	–	3305	–	1596	–	609	1319 (1327)	–	–	–
		(3470)	(3302)	(3162)	(1634)	(809)	(–)				

Values between parentheses are the ligand bands.

Table 3
Electronic spectral data of Pt(IV) complexes

Compound	State	Charge transfer and intraligand bands (cm^{-1})		
$[Pt(AT)_2(H_2O)_2]Cl$	DMF	20,780	–	28,735; 30,675
$[Pt(AET)Cl_3]PtCl_4$	DMF	–	24,096	27,855
$[Pt(APT)(H_2O)(C_2H_5OH)Cl_3]$	DMF	–	23,474	27,780; 31,745
$[Pt(ST)(OH)Cl]0.5H_2O$	DMF	–	24,095	28,090
$[Pt(H_2SET)Cl_3]Cl{\cdot}3H_2O$	DMF	–		26,455
$[Pt(SPT)(C_2H_5OH)Cl_2]$	DMF	–	–	26,810; 30,865
$[Pt(HyMBPT)Cl_2]$	DMF	21,210	24,210	27,030

Pt(IV) complexes. The electronic spectra of the ligands in DMF show $\pi \rightarrow \pi^*$ band at 32,790–40,820 cm^{-1} and $n \rightarrow \pi^*$ band at 28,570–30,960 cm^{-1}; little change is observed on the spectra of their complexes with a new $n \rightarrow \pi^*$ band at 27,000–28,250 cm^{-1}. The band at 22,680–24,040 cm^{-1} in the spectra of the complexes may be due to LMCT. Previous studies on thiosemicarbazone complexes proved that the band in the region 25,000–26,040 cm^{-1} is assignable to $S(\sigma) \rightarrow Cu(II)$ transition, the 20,600 cm^{-1} band is due to $S(\Pi) \rightarrow Cu(II)$ transition [22,23] whereas the band at 21,790–24,750 is due to $O \rightarrow M(II)$. Table 3 shows the spectral bands of the investigated complexes. The spectra displayed charge transfer and spin allowed transitions correlated with an octahedral geometry [24].

3.3. Mass spectra

The mass spectra of some complexes are recorded and the obtained molecular ion peaks confirm the proposed formulae. The found and calculated molecular weights are presented in Table 1. The mass spectrum of $[Pt(ST)(OH)Cl]0.5H_2O$ shows quartet peak at 449, 450, 451 and 452 with 2.39, 7.49, 4.21 and 3.85% abundances, respectively. The one at 450 may represent the molecular ion peak of the complex; the others are isotopic species. The formula of the complex contains half water molecule which may exist in hydrogen bonding with the complex and removed with the OH in the first step leaving a peak at 425. The strongest peak (base beak) at *m/e* = 169 represents the stable species $C_7H_5NO_2S$ after which multipeaks are observed ending with 4C at *m/e* = 50 with 22% abundance.

The second example is the ms of [Pt(HyMBPT)Cl] (Fig. 1) which exhibits triplet peak at 638 (8.92%), 639 (14.48%) and 640 (10.84%) representing the molecular ion peak, $C_{21}H_{17}PtN_3O_3SCl_2$. The second peak at *m/e* 416 represents the removal of $C_7H_5N_2SCl_2$ after which Pt metal is removed. The base peak at *m/e* 78 represents C_6H_5 moiety.

3.4. Thermal studies

The TG thermograms of some complexes were studied in the temperature range 30–800 °C. The data of all decomposition steps are collected in Table 4. As shown the complexes are not decomposed completely. It is observed that the complexes are stable except $[Pt(H_2SET)Cl_3]Cl{\cdot}3H_2O$ in which its first decomposition step at 23–91 °C represents the removal of one of the water molecule. As a representative example for the decomposition of these complexes, the TG of $[Pt(HyMBPT)Cl_2]$ shown in Fig. 2 is described. The complex is stable till 194 °C and its thermogram reveals two main decomposition stages. The $C_{13}H_{11}N_2Cl_2$ moiety may be eliminated in the first step which is major (Found 40.7, Calcd. 41.6%). The second step suggests the

Table 4
Thermogravimetric data of some investigated complexes

Complex	Temperature (°C)	Species removed	Found (Calcd.) (%)
$[Pt(APT)(H_2O)(C_2H_5OH)Cl_2]Cl$, $C_{17}H_{22}PtN_3O_2SCl_3$	194–329	$-(C_2H_5OH + H_2O + Cl_2)$	21.1 (21.3)
	330–412	–Cl	4.6 (5.6)
	413–541	$-(CH_3 + C_7H_6N_2)$	21.4 (21.0)
	542–800	$[Pt(C_7H_5NS)]$	53.8 (52.0)
$[Pt(ST)(OH)Cl]0.5H_2O$, $C_8H_9PtN_3O_{2.5}SCl$	174–244	$-(0.5H_2O + Cl + OH + NH_2)$	16.2 (17.2)
	245–342	–CN	7.4 (6.0)
	343–517	$-C_7H_5$	17.1 (20.0)
	518–800	[PtNOS]	59.3 (57.2)
$[Pt(H_2SET)Cl_3]Cl{\cdot}3H_2O$, $C_{10}H_{18}PtN_3O_4SCl_4$	23–91	$-H_2O$	2.5 (2.9)
	92–203	Stable	–
	204–416	$-(2H_2O + 3Cl)$	21.7 (22.8)
	417–629	$-(Cl + C_2H_5)$	9.8 (10.4)
	630–800	$[Pt(C_8H_7N_3SO)]$	62.6 (62.5)
$[Pt(SPT)(C_2H_5OH)Cl_2]$, $C_{16}H_{17}PtN_3O_2SCl_2$	210–300	$-(C_2H_5OH + C_6H_6N)$	25.4 (23.9)
	301–408	$-Cl_2$	12.9 (12.3)
	409–555	$-C_8H_5N$	22.0 (19.9)
	556–800	[PtNOS]	44.1 (44.6)

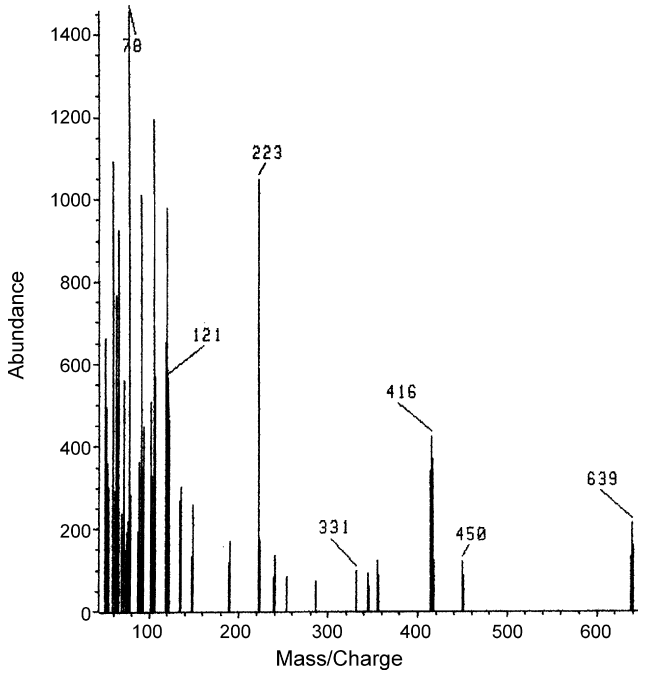

Fig. 1. The mass spectrum of [Pt(HyMBPT)Cl_2].

expulsion of $C_8H_6NO_2S$ (Found 28.3, Calcd. 29.1%). A continuous decomposition is taking place until 800 °C. The residue is Pt (Found 30.9, Calcd. 30.4%).

3.5. Antimicrobial activity bioassay

The antimicrobial activity of some investigated ligands and complexes against *Sarcina* sp. and *E. coli* is summarized in Table 5. The ligands are H_2HyMB*p*CPT (3), H_2ST (6), H_2*o*HAT (9) and H*p*NAT (10), where the complexes are [Pt(H_2SET)Cl_3]Cl·3H_2O (1), [Pt(SPT)(C_2H_5OH)Cl_2] (2), [Pt(HyMBPT)Cl_2] (4), [Pt(ST)(OH)Cl]0.5H_2O (5), [Pt(*p*NAT)Cl_3(H_2O)] (7) and [Pt(*o*HAT)(OH)Cl] (8). Growth inhibition zones are proportional to the antimicrobial activity of the tested compound. The data suggest that Gram-negative bacterium (*E. coli*) was less affected by the tested chemicals

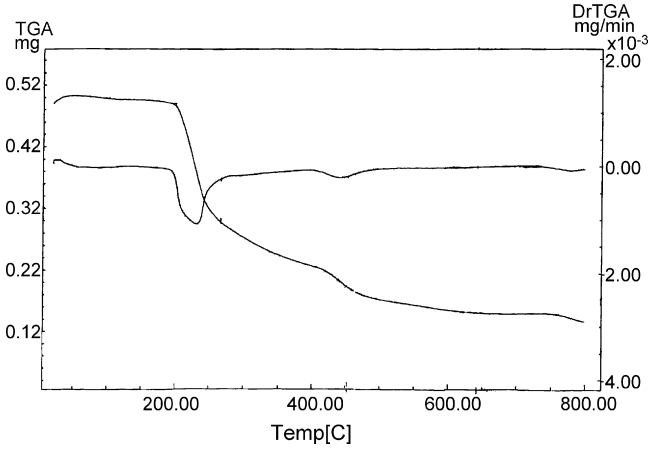

Fig. 2. The TG and DrTG thermograms of [Pt(HyMBPT)Cl_2].

Table 5
Antimicrobial activity of the tested compounds

Compound	Diameter of growth zone of inhibition (mm)	
	E. coli	*Sarcina*
[Pt(H_2SET)Cl_3]Cl·3H_2O (1)	0	0
[Pt(SPT)(C_2H_5OH)Cl_2] (2)	0	8
H_2HyMBPT (3)	0	21
[Pt(HyMBPT)Cl_2] (4)	0	7
[Pt(ST)(OH)Cl]0.5H_2O (5)	0	0
H_2ST (6)	0	10
[Pt(*p*NAT)(H_2O)Cl_3] (7)	12	32
[Pt(*o*HAT)(OH)Cl] (8)	18	34
H_2*o*HAT (9)	0	25
H*p*NAT (10)	0	8

than the Gram-positive bacterium (*Sarcina*). Compounds number 3, 7, 8 and 9 are more potent in killing *Sarcina* sp. than the others because of their relatively large zones of growth inhibition. Also, compounds 7 and 8 exhibited low to moderate inhibition on the growth of *E. coli* which can be classified to wide host range because of their activity against Gram-positive and Gram-negative bacteria. On the other hand, compounds 2, 3, 6 and 9 are only active against Gram-positive bacteria, i.e. have narrow host range. The compounds may be arranged according to their activity against *Sarcina* as: [Pt(*o*HAT)(OH)Cl] > [Pt(NAT)(H_2O)Cl_3] > H_2*o*HAT > H_2HyMB*p*CPT > H_2ST > [Pt(SPT)(C_2H_5OH)Cl_2] > H*p*NAT > [Pt(ST)(OH)Cl]0.5H_2O (5). It is observed also that *o*-hydroxyacetophenone thiosemicarbazone and its complex (Scheme 2) have higher activity against *E. coli* than the other compounds. The sixth coordination position is vacant and may be occupied and the complex may act as a co-enzyme.

3.6. Eukaryotic DNA degradation test

Examination of the electrophoretic mobility (Fig. 3) of all treatments in comparison to the control sample revealed that no change in lanes 1, 2 and 3, whereas, slight downward shifts in mobility are observed in lanes 4–10, and this was associated with tailing of the DNA. Electrophoretic mobility shift and tailing of DNA in any lane are indicative of the degradation of calf thymus DNA. It is important to note that DNA degradation and antimicrobial activity against Gram-positive bacteria coincided real well. However, the degradation powers of the tested chemicals on the calf thymus DNA were very slight. This would support

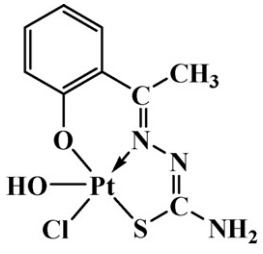

Scheme 2. Structure of [Pt(*o*HAT)(OH)Cl].

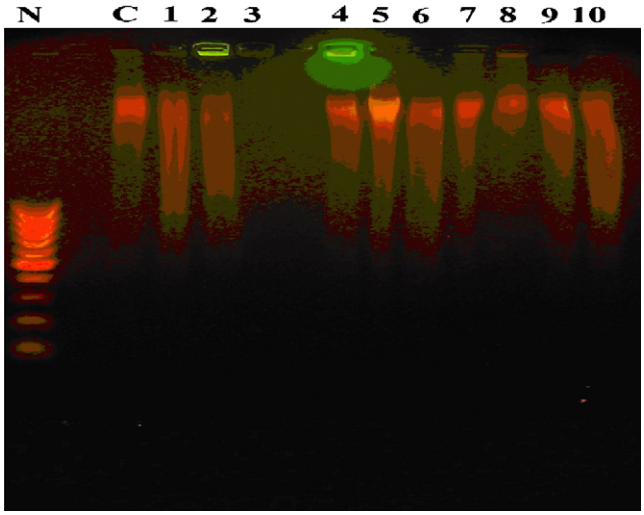

Fig. 3. The effect of ligands and complexes on calf thymus DNA; panel N, DNA molecular weight marker; panel C, calf thymus DNA control sample; panels from 1 to 10, calf thymus DNAs treated with ligands and complexes.

the selective action of these compounds against bacteria and not against the human or related eukaryotic organism.

4. Conclusion

The complexation between H_2PtCl_6 and the investigated thiosemicarbazones proceed by the same technique but with different modes of coordination depending on the substitutent group. Most complexes are thermally stable and completely undecomposed. The antimicrobial activity shows that some compounds are more potent in killing *Sarcina* sp. Electrophoretic mobility of all treatments revealed slight shifts in lanes 4–10. The data of antimicrobial activity against Gram-positive bacteria agree well with those of DNA degradation.

Appendix A. Supplementary data

Supplementary data associated with this article can be found, in the online version, at doi:10.1016/j.saa.2007.03.010.

References

[1] E. Jouad, A. Riou, M. Allain, M.A. Khan, G.M. Bouet, Polyhedron 20 (2001) 67.
[2] D.X. West, J.K. Swearingen, J.V. Martinez, S.H. Ortega, A.K. El-Sawaf, A. Meurs, A. Castineiras, I. Garcia, A. Bermejo, Polyhedron 18 (1999) 2919.
[3] L.J. Ackerman, P.E. Franwick, M.A. Green, E. John, W.E. Running, J.K. Swearingen, J.W. Webb, D.X. West, Polyhedron 18 (1999) 2759.
[4] M.C. Miller, C.N. Stineman, J.R. Vance, D.X. West, I.H. Hall, Anticancer Res. 18 (1998) 4131.
[5] P. Bindu, M.R.P. Kurup, Ind. J. Chem. 38 (1999) 388.
[6] R.P. John, A. Sreekanth, M.R.P. Kurup, S.M. Mobin, Polyhedron 21 (2002) 2515.
[7] A.A. Nassar, F.A. El-Saied, M.I. Ayad, D.X. West, Transition Met. Chem. 24 (1999) 617.
[8] D.X. West, Y.H. Yang, T.L. Klein, K.I. Goldberg, A.E. Liberta, J. Martinez, S. Hernandez-Ortega, Polyhedron 14 (1995) 1681.
[9] D.X. West, H. Gebremedin, R.J. Butcher, J.P. Jasinski, A.E. Liberta, Polyhedron 12 (1993) 2489.
[10] R.M. El-Shazly, G.A.A. Al-Hazmi, S.E. Ghazy, M.S. El-Shahawi, A.A. EI-Asmy, Spectrochim. Acta 61 (2005) 243.
[11] G.A.A. Al-Hazmi, M.S. El-Shahawi, A.A. El-Asmy, Transition Met. Chem. 30 (2005) 464.
[12] N.M. EI-Metwally, R.M. El-Shazly, E. Gabr, A.A. El-Asmy, Spectrochim. Acta 61 (2005) 1113.
[13] G.A.A. Al-Hazmi, M.S. El-Shahawi, I.M. Gabr, A.A. El-Asmy, J. Coord. Chem. 58 (2005) 713.
[14] A.A. Abou-Hussain, N.M. El-Metwally, E.M. Saad, A.A. El-Asmy, J. Coord. Chem. 58 (2005) 1735.
[15] D.D. Perrin, W.L.F. Armorego, Purification of Laboratory Chemicals, third ed., Pergamon Press, 1988.
[16] A.I. Vogel, A Text Book of Quantitative Inorganic Analysis, Longmans, London, 1994.
[17] S.D. Dhumwad, K.B. Gudasi, T.R. Goudar, Ind. J. Chem. 33(A) (1994) 320.
[18] S.K. Sengupta, O.P. Pandey, A. Rai, A. Sinha, Spectrochim. Acta (A) 65 (2006) 139.
[19] I.T. Ahmed, Spectrochim. Acta (A) 65 (2006) 5.
[20] A. Rai, S.K. Sengupta, O.P. Pandey, Spectrochim. Acta (A) 64 (2006) 789.
[21] M. Gabryszewski, Spectrosc. Lett. 34 (2006) 57.
[22] A.B.P. Lever, Inorganic Electronic Spectroscopy, Elsevier, Amsterdam, 1986.
[23] J.P. Jasinski, J.R. Bianchani, J. Cueva, F.A. El-Saied, A.A. El-Asmy, D.X. West, Z. Anorg, Allg. Chem. 629 (2003) 202.
[24] G. Ponticelli, A. Spanu, M.T. Cocco, V. Onnis, Transition Met. Chem. 24 (1999) 370.